Non-spherical Toner Behavior Simulation by Polyhedral Particle

Toyoshige Sasaki[1], Shingo Nagai[1], Masanori Shida[2], Yasuo Yoda[3]
[*]1 Analysis Technology Center, Canon Inc., Tokyo, Japan
[*]2 Office Imaging Products Device Development Center, Canon Inc., Ibaraki, Japan
[*]3 Peripherals Development Center, Canon Inc., Shizuoka, Japan

Abstract

The shape of toner particles has a significant influence on the imaging performance in the electro-photographic process. In this study, we developed a program that calculates the toner behavior as we considered every particle shape. The program uses a distinct element method using polyhedral particles. We developed algorithms that classify the contact of the particle into four patterns depending upon the tangency of the vertex, the edge and the face of polyhedron. Utilizing the developed program, we calculated how the toner scatters by creeping discharge. Furthermore, we investigated the reason why a sphere toner scatters more intensely than non-sphere toner. As a result, we found that the difference between toner's shapes and adhesive properties in terms of their motion flexibility determines the scattering performance.

Introduction

During the electro-photographic process, the shape of toner particles plays a critical role in the image performance. Hence, the simulation must be able to consider the toner shape. Generally, for the crowded toner behavior calculation, the distinct element method (DEM) is used. The DEM frequently adopts sphere particles as its elements [1]. Another way to calculate such behavior, without using spherical elements, is Cundall's method. Cundall's study [2],[3] uses polyhedral elements instead of spherical ones. This study compares two approaches to examine one of the essential procedures during the DEM, which is to find the contact of two particles. One of which, called the direct approach, directly examines the contact of polyhedron particles. The other, called the indirect approach, utilizes a plane (common-plane) to examine the contact. This study concludes that the latter, the indirect approach, results in better calculation speed, robustness and process simplicity than the former, the direct approach. However, the algorithm of the direct approach is flexible and that it leaves room for improvement. In this study, we further developed the direct approach and applied the method to develop a program that would calculate the toner behavior.

Simulation Method

Our developed program uses polyhedrons to represent particles. When a particle contacts with another object, the program calculates the contact force by spring force, damper force and slider friction force. These conditions are the same under the usual DEM. Then, the program calculates each particle's behavior by solving the motion equation. When calculating contact force, the Hertzian contact stress is used and the radius of the sphere is determined by the minimum sphere radius which involves the particle. Figure 1 shows an example of a polyhedral particle. For simplicity, only convex shapes are considered in this report. Descriptions for the characteristics of the polyhedron particle in this study are the following.

Classification of Contact

This study explains the contact force calculation process by using an example of the hexahedron particle case. Figure 2 shows how part of particle-*i* penetrates particle-*j*. We classified the tangency of two particles into four patterns as (a), (b), (c) and (d). Upper figures show each penetration pattern in three dimensions, and lower figures show two particles' penetrating statuses in a schematic model. In these figures, solid lines represent particle-*i*, dotted lines represent particle-*j*, and i-v_0, i-e_0, i-f_0 represent vertex v_0 , edge e_0, face f_0 of particle-*i*, respectively. The star mark stands for the point where the vertex or edge of particle-*i* penetrates particle-*j* (call this point "penetrating point"). The black circle represents the edge of particle-*j*, and the δ shows the penetration quantity of particle-*i* to particle-*j* in lower figures. Each penetration pattern is explained as follows.

(a) Vertex to Face Penetration: This is the case where a vertex of particle-*i* penetrates a face of particle-*j*. When the vertex of particle-*i* is inside the particle-*j*, two particles are assumed to be in contact. The vertex i-v_0 penetrates the face j-f_0 in this figure. In this case, vertex i-v_0 is defined as the penetrating point. Then the distance between the vertex i-v_0 and the face j-f_0 is the penetration quantity. We call the face j-f_0 "penetration base face".

(b) Vertex Edge to Face Penetration: This is the case where an edge of particle-*i*, whose vertex is penetrating, also penetrates an edge of particle-*j* in addition to case (a). We call this edge, whose vertex is penetrating, "vertex edge". When considering the vertex edge of case (a), so long as the number of crossing point(s) is one and the face which contains the crossing point(s) is not the penetration base of (a), the case falls into this category. In the figure, vertex i-v_0 is penetrating face j-f_0, and so is vertex edge i-e_0 penetrating j-e_0. In this examination, the crossing point of vertex edge i-e_0 and face j-f_1 (call this point P) are also considered the penetrating point in addition to case (a). And the distance between the face j-f_0 and the point P is the penetration quantity.

(c) Edge to Edge Penetration: This is the case where an edge

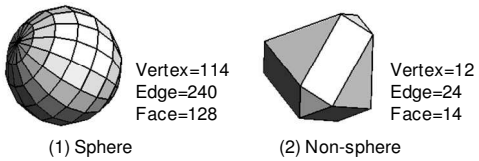

Figure 1. *Polyhedral particle model*

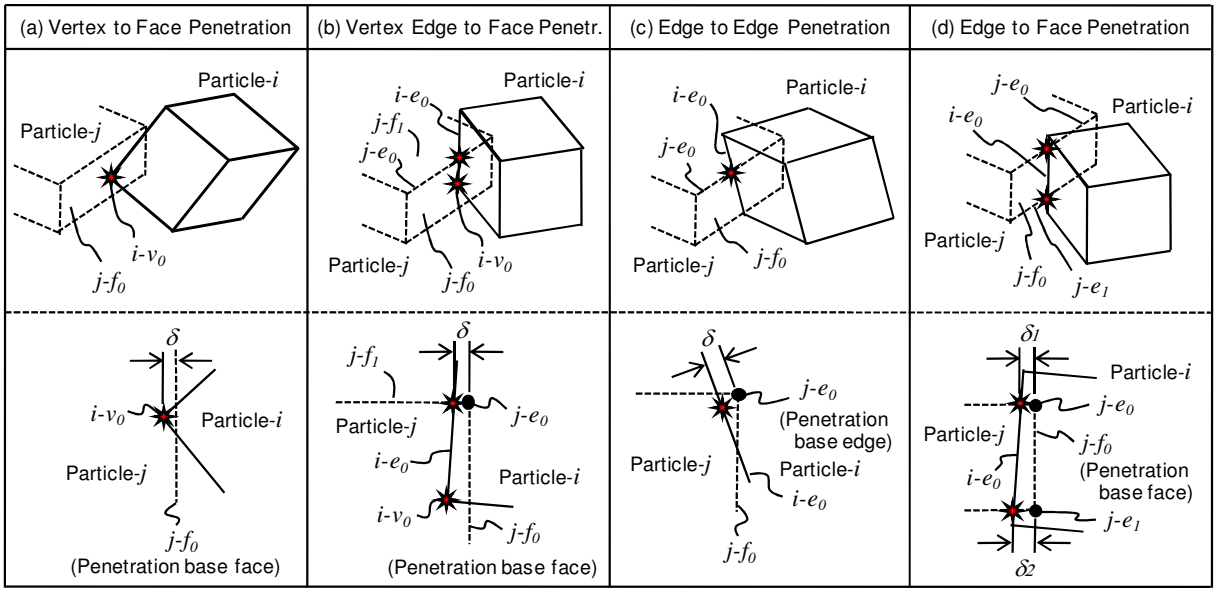

Figure 2. *Two particles contact pattern*

of particle-*i* penetrates an edge of particle-*j*. Typically when the edge i-e_0 crosses two faces of particle-*j* and two edges, which are nearest to the crossing point on each faces, are the same, the contact corresponds to this case. The edge i-e_0 penetrates the edge j-e_0 in this figure. In this case, the point on the edge i-e_0, the nearest point to the edge j-e_0, is assumed the penetrating point. And the distance between the edge j-e_0 and the edge i-e_0 is the penetration quantity. We call the edge j-e_0 "penetration base edge".

(d) Edge to Face Penetration: This is the case where an edge of particle-*i* penetrates two edges of particle-*j*. When an edge i-e_0 crosses two faces of particle-*j* and case (c) does not apply, the contact is classified as this case. The edge i-e_0 penetrates the edge j-e_0 and edge j-e_1 in this figure. In this case, the two points where the edge i-e_0 crosses the faces of particle-*j* are assumed the penetrating points. We define one of the particle-*j*'s faces, nearest to the two penetrating points (when sum of distances between the penetrating point and the faces becomes the minimum), as "penetration base face". In the figure, the face j-f_0 is the penetration base face. And the both distances between each penetrating point and base face are the penetration quantity.

During the actual program's run, when case (a) or (b) is applied and the vertex i-v_0 penetrates near/around the edge of particle-*j*, a special process is proceeded to maintain the force direction validity and force magnitude continuity. Likewise, this process is done when case (c) or (d) is applied and the edge i-e_0 penetrates near/around the vertex of particle-*j*. However in this report, to avoid confusion, these details have been omitted.

Contact Force Calculation Method and Flow

Depending on the penetration quantity, the program adds the Hertzian contact stress at the penetration point found in the earlier process. In case (a), (b) and (d), the force direction goes from the penetrating point to the penetration base face. In case (c), the force direction goes from the penetrating point to the nearest point on penetration base edge. Figure 3 shows the calculation flow, which

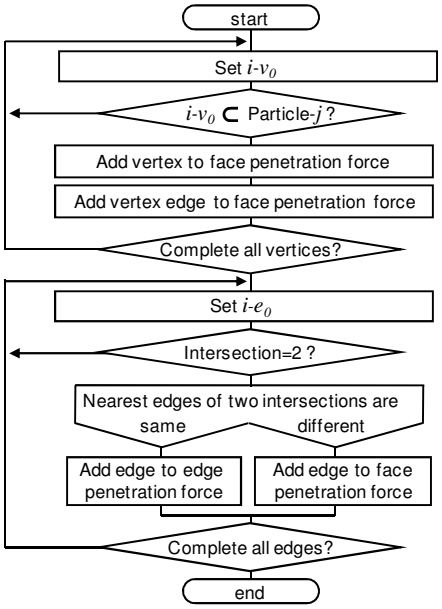

Figure 3. *Particle-i force calculation flow*

integrates the contact judge method. The vertex penetration contact force is calculated in the first half, and the edge penetration contact force is calculated in the rest. The program also adds friction force at the penetrating points by the same method as the conventional DEM. The particles behavior is calculated by the contact force acting as both translation movement force and rotation movement force.

Validity of Contact Model

The following are the problems found in the polyhedrons contact force calculation model above.

(1) Contact Mode: Generally the particle contact occurs as a point, line or area. For example, Figure 2 (b) and (d) occurs as a

line contact. In this contact model, contact mode is simplified to a plural point contact shown in stars.

(2) Hertzian Contact Stress: Though the actual contact areas do not appear spherical, Hertzian contact stress - the equation used when a sphere contacts with another - is used to calculate the contact force.

(3) Polygon Fineness Dependence: The model considers cases where two particles penetrate one another with a constant penetration quantity. As the penetrating area becomes finer in polygon, the number of penetrating vertices and edges increase. As a result, the contact force becomes bigger as the polygons become finer.

Our thoughts regarding these problems are discussed below.

For (1), we acknowledge that this contact model may not always be physically accurate, but this model produce acceptable results in terms of finding the effects of particle shapes.

For (2) and (3), we limited the calculation problems only to the cases where the toner movements are slow. This limitation should not invalidate the accuracy of the examination based on the fact that toner's motion is active only when the toner is dense. Furthermore, a significant amount of air viscosity force works on each active toner particle. Regarding this limitation, one must consider spring force and damper force since they are the main sources of contact force. Spring force is a force that works with respect to penetration quantity. The problem of our particle spring model is that the model often makes two kinds of errors: penetration quantity errors and natural frequency errors. For penetration quantity errors, though penetration quantity does not always correspond to the actual phenomena, the results for the toner behavior are correct. This is because the spring force, calculated from the penetration quantity, is correct. Hence, these errors can be disregarded. For natural frequency errors, since the toner motion is slow, these errors have little effect on toner behavior. Damper force is a force that works with respect to the change of penetration quantity. Because damper force is considerably smaller than spring force when the particle motion is slow, the effect that damper force have against toner behavior is insignicant. For these reasons, the problem (2) and (3) do not invalidate the program's results unless the toner collides so fast that the rebound motion weakens its accuracy, which could only be caused by a strong electric field and such extreme cases.

Creeping Discharge Toner Scattering

The toner receives a separating discharge and sometimes scatters in the transfer process. The degree of the scattering depends on the toner shape. Utilizing the developed program, we calculated the scattering of spherical toner and non-spherical toner by creeping discharge. And we investigated the causes of scatter difference.

Creeping Discharge Pattern

We examined the difference of scattering between spherical toner and non-spherical toner by separating discharge in Figure 4. For this examination, toner is transferred to the paper on the middle electric resistance transfer belt while separating the paper from the belt and, then, implementing the fixing process. Figure 5 shows the obtained image. A twig-like electrical discharge pattern is found in the spherical toner image. On the other hand, there is

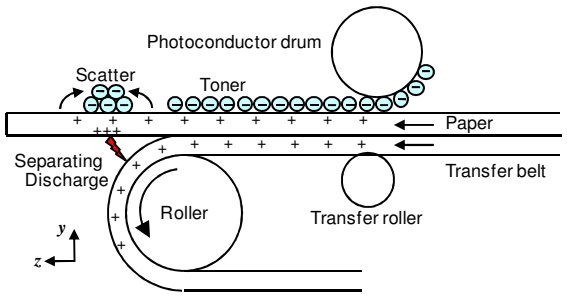

Figure 4. *Separating discharge experiment system*

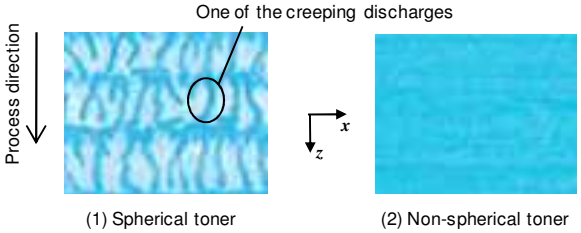

Figure 5. *Scattered toner image(experiment)*

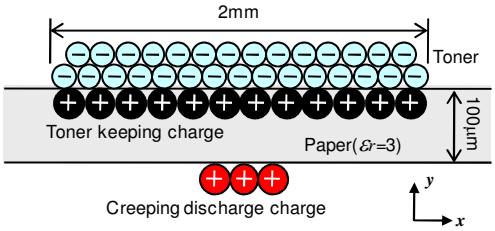

Figure 6. *Simulation model*

Table 1. Material Properties

Properties	Paper	Toner
Young's modulus(MPa)	6000	3200
Poisson's ratio(-)	0.3	0.3
Restitution coefficient(-)	0.2	0.3
Friction coefficient(-)	0.6	0.2/0.6
Adhesion force[nN]	10/100	

no prominent pattern found in the non-spherical toner image. Only lights and shades are detected. This pattern represents a positive creeping discharge pattern. When the paper charged with a negative charge separates from the belt, it receives a separating positive discharge. The found pattern is created by this reaction.

Simulation Model

We calculate the twig, shown in the positive creeping discharge pattern, by the simulation. Figure 6 shows the simulation model. This model requires a condition where tonner particles are randomly accumulated on the paper and the toner keeping charge is arranged around the surface of the paper. The toner behavior is calculated when the amount of the charge, placed in the back center area of the paper, weighs equivalent to the amount of the

creeping discharge charge. The analytical area length in the direction of the figure depth is 120μm, and the cyclic boundary condition is the both boundary faces. The main properties are shown in Figure 6. Both the toner keeping charge and the creeping discharge charge are expressed in the arranging immovable particles with charge.

The two toner particles shown in Figure 1 are used in the calculation. The size of the particle is defined by the diameter of its circumscribing sphere, and the size distribution is assumed to coincide with gauss distribution. The median diameter, the standard deviation, the minimum diameter, and the maximum diameter are 6.7μm, 1.6μm, 4.1μm, 10.2μm respectively for the spherical toner, and 8.6μm, 2.1μm, 5.2μm, 13.0μm respectively for the non-spherical toner. The volume distribution of the spherical particle and the non-spherical particle are made equivalent by adjusting the particle diameter.

The specific gravity, the relative permittivity, the charge-to-mass ratio (Q/M), and the amount (M/A) regarding toner characteristics are 1.2, 2.0, -20μC/g, and 0.6mg/cm^2 respectively and the particle count is 8,190 for both spherical and non-spherical case. The charge density of the arranged toner layer is -120μC/m^2, and the toner keeping charge is set to 80μC/m^2. Table 1 shows the physical property values of each paper and toner. Gaussian distribution is used to illustrate the density of spatial creeping discharge charge. This distribution's peak value is set to 1,000μC/m^2 or 3,000μC/m^2 and the FWHM is 94μm. The time step and the iteration count is 2.5nsec and 1,400,000, respectively.

Result and Discussion

Figure 7 shows numerical results of toner scattering when the creeping discharge charge density is modified. This figure is the top view of the paper. The toner friction co-efficient is assumed 0.2, and the toner adhesion force is 10nN. When the discharge charge density is 1,000μC/m^2, the scatterings of both toner shapes are small. When the discharge charge density is 3,000μC/m^2, all toner perfectly gathers around the creeping discharge charge in the spherical toner result. However on the other hand, some toner remains in the non-spherical one. The difference is occurred from the fact that the spherical toner can translate smoothly by rotating, but the non-spherical toner cannot. Although the difference can be observed in these calculation results, the difference doesn't appear as obvious as the experimental results shown in Figure 5.

To find out what causes the difference in intensity of scattering between spherical and non-spherical toner, the examination for changes of toner scattering is conducted. This examination is done under a condition where a friction co-efficient and adhesion force increase because this seemed to have affected the particle movement flexibility. The scatter was compared at the discharge charge density being 3,000μC/m^2. Figure 8 shows the results. Though the scatter is reduced by increasing the friction co-efficient to 0.6, the change is small. On the other hand, the scatter is remarkably reduced by increasing the adhesion force to 100nN.

The toner particles are compressed at the transfer nip, and the adhesion force increases. It is thought that the adhesion force of non-spherical toner is bigger than that of spherical toner. We think the cause, which makes the sphere toner scatter more intensely than non-sphere toner, is flexibility of particle movement with regard to its shape and its adhesion force.

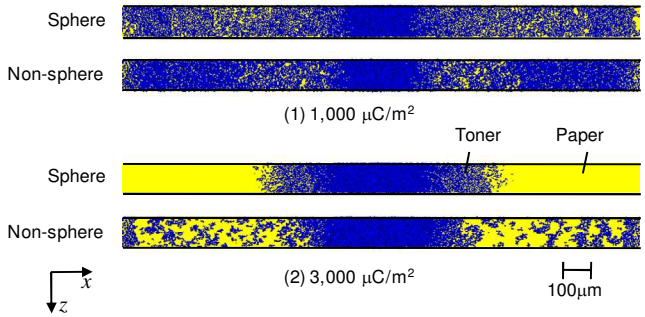

Figure 7. *Calculation result of toner scattering depend on peak charge density of the creeping discharge (Friction coefficient=0.2, Adhesion force=10nN)*

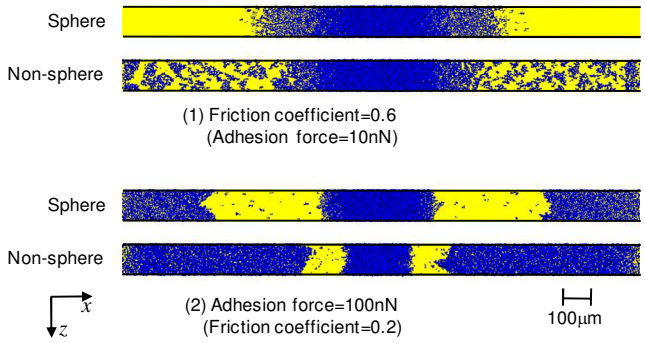

Figure 8. *Toner scattering depend on the toner friction and the toner adhesion force. (Creeping discharge charge density=3,000 μC/m^2)*

Conclusion

We developed a program that calculates the toner behavior as we considered every particle shape. Utilizing the developed program, we investigated the cause on the particle shape dependency of the toner scattering by creeping discharge.

References

[1] S. Nagai, T. Sasaki, and M. Nakano: A Study on Behavior of Magnetic Particles using Discrete Element Method, Japan Hardcopy '99, 185-188 (1999) [in Japanese]

[2] P.A. Cundall: Formulation of a three-dimensional distinct element model □ Part I. a scheme to detect and represent contacts in a system composed of many polyhedral blocks, Int. J. Rock Mech. Min. Sci. & Geomech. Abstr., 25(3), pp.107-116 (1988)

[3] R. Hart, P.A. Cundall, and J. Lemos: Formulation of a three-dimensional distinct element model □ Part II. mechanical calculations for motion and interaction of a system composed of many polyhedral blocks, Int. J. Rock Mech. Min. Sci. & Geomech. Abstr., 25(3), pp.117-125 (1988)

Author Biography

Toyoshige Sasaki received his B.S. and M.S. degrees from Waseda University, Japan in 1982 and 1984, respectively. He joined Canon in 1984 and has been engaged in the development of electromagnetic devices such as electromagnetic actuators for cameras and electro-photographic processes by using numerical simulations.